Compressed SUSY searches with Monojet events at CMS

Robyn Elizabeth Lucas
Imperial College London

A dissertation submitted to Imperial College London
for the degree of Doctor of Philosophy

Abstract

This is the abstract, find me in frontmatter.tex

Declaration

This dissertation is the result of my own work, except where explicit reference is made to the work of others, and has not been submitted for another qualification to this or any other university. This dissertation does not exceed the word limit for the respective Degree Committee.

Robyn Lucas

Acknowledgements

Mr Darcy and Mr Merlin deserve particular thanks.

Preface

This thesis describes my research on various aspects of the CMS particle physics program, centred around the CMS detector and LHC accelerator at CERN in Geneva.

For this example, I'll just mention Chapter **??** and Chapter **??**.

Contents

"For Peter"

—

Chapter 1.

Introduction

"Everything starts somewhere, although many physicists disagree."
— Terry Pratchet

Chapter 2.

Theory and Motivations

"Absence of evidence is not evidence of absence."
— Carl Sagan, 1934 - 1996

The Standard Model (SM) of particle physics provides a fabulously accurate description of the most fundamental forces and particles known to exist. It has been shown to be robust beyond measure in the first years of running at the LHC. In this chapter I discuss the theory of the SM, its successes and failings, and motivate a Supersymmtric extension of the SM.

2.1. The Standard Model of Particle Physics

2.1.1. Gauge Symmetries

2.1.2. Electoweak Symmetry Breaking

2.2. Motivation for Physics Beyond the Standard Model

2.3. Supersymmetry

2.3.1. Compressed Supersymmetry

Chapter 3.

The LHC and CMS experiment

"Insanity: doing the same thing over and over again and expecting different results."

— Albert Einstein, 1879 - 1955

Probing the physics of the Standard Model (SM) and beyond at the TeV scale is only possible with the technologically unparalleled apparatus situated at the European Organisation for Nuclear Research (CERN). This chapter will introduce the hugely complex machinery of the LHC, which provides proton-proton collisions at energies in excess of $\sqrt{7}$ TeV, and outline the main features of the Compact Muon Solenoid (CMS) experiment, of which the author is a member, with particular focus on those features relevant to the material presented in this thesis. Section 3.1 presents the main features of the Large Hadron Collider (LHC), and Section 3.2 provides an overview of the CMS detector.

3.1. The LHC

The LHC is the world's largest and most energetic synchrotron particle collider. Housed in the tunnel built for the Large Electron-Positron Collider (LEP) collider that operated during the 1990's at CERN, the LHC is a double ring circular collider 27 km in circumference, and sits on the bedrock beneath the Franco-Swiss border, close to Geneva, Switzerland. It is designed for both proton-proton (pp) and heavy ion (PbPb) collisions at a centre of mass energy $\sqrt{s} = 14$ TeV and luminosity of $10^{34}\text{cm}^{-2}\text{s}^{-1}$.

Currently the world's only operating collider able to study physics at the TeV scale, the LHC consists of thousands of superconducting magnets which act to accelerate, bend and focus two beams of protons (or heavy ions) that circulate in opposite directions around the accelerator. A chain of accelerators, culminating with the Super Proton Synchrotron (SPS), inject bunches of approximately one hundred billion protons 25 or 50 ns apart at $\sqrt{s} = 450$ GeV into the two beams of LHC. Oscillating electric fields provided by 1232 superconducting dipole magnets act to accelerate the beams up to the operating centre of mass energy, which for the data used in this thesis was $\sqrt{s} = 8$ TeV, with bunch crossings every 50 ns. Once protons are accelerated to the operational $\sqrt{s}$, the LHC acts as a storage ring, and collisions can occur. Either side of four points around the LHC ring, very high precision magnetic fields, provided by quadrupole and higher order multipole magnets, position and focus the beams such that each bunch has a diameter of 16 μm. The chance of a pp collision with large momentum transfer at the four interaction points around the LHC ring is thereby increased, and the number of such collisions per bunch crossing, termed "pile-up" (PU) for the data used in this thesis was ~ 20.

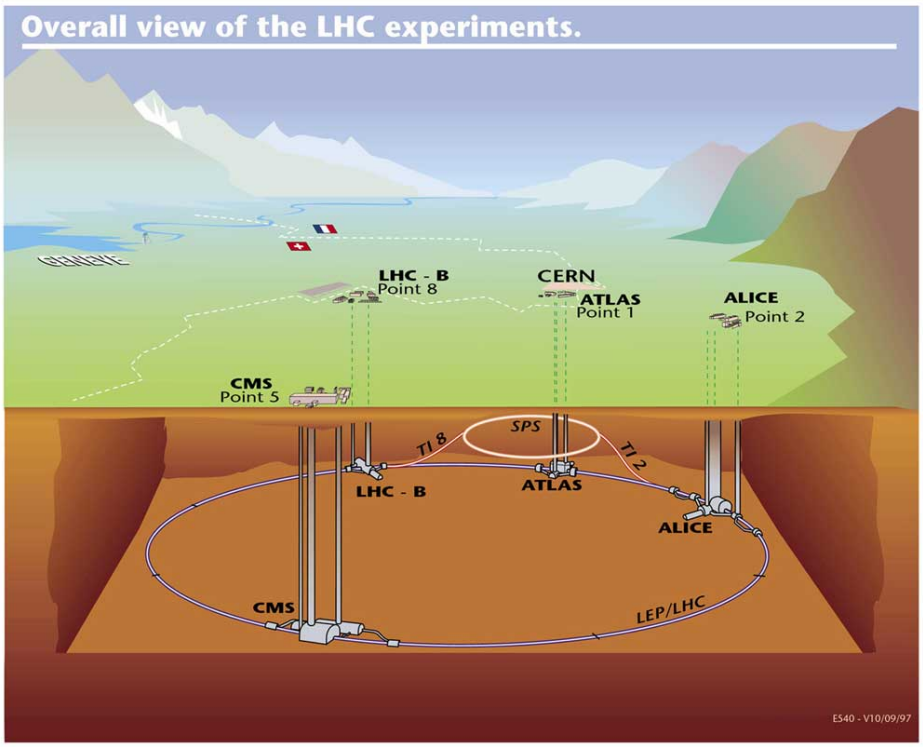

Figure 3.1.: The LHC accelerator ring, showing the locations of the four main experiments at the four collision points.

Interaction points are at the centre of four large particle detectors, shown in Figure 3.1: A Large Ion Collider Experiment (ALICE) [1], A Large Toroidal LHC ApparatuS (ATLAS) [2], Compact Muon Solenoid (CMS) [3] and Large Hadron Collider Beauty (LHCb) [4]. They act to identify particles produced as a result of a pp or PbPb bunch crossing through a combination of tracking and calorimetry, in order to reconstruct and measure physical processes, to test currently accepted theories and search for new physics.

3.2. The CMS Detector

The CMS detector is a general purpose particle detector, designed to carry out many different measurements for various physics goals. Close to 4π reconstruction with efficient particle identification and reconstruction allows measurements of photons, muons, electrons, taus, hadronic showers and missing transverse momentum. A diagram of CMS is shown in Figure 3.2. It is 21.6 m long, 14.6 m in diameter and weighs 12500 T. It consists of different sub-detectors, each of which measures a different particle or property, and is built around a central 12.5 m long 4 T superconducting solenoid magnet and its iron return yoke. CMS consists of a barrel region, containing the solenoid, and endcaps to extend the forward and backward coverage.

The different sub-detectors are arranged in an onion structure. Closest to the beam line is the silicon tracking system. A very highly resolution pixel detector lies closest to the interaction region, followed by a granular strip detector. Charged particle momenta measurements are made using the curvature of tracks in the uniform magnetic field provided by the solenoid, as well as measurements of displaced vertices and impact parameters which are essential for identifying heavy flavor decays. Energy measurements are provided by the calorimeters, which lie outside of the tracker; the Electromagnetic Calorimeter (ECAL) and Hadronic Calorimeter (HCAL). The highly granular ECAL consists of 70,000 transparent lead tungstate crystals, which allow accurate electron and photon position and energy measurements. Scintillation light produced in the crystals is collected by photodetectors and used to infer the incident particle energy. The sampling HCAL consists of slabs of brass interleaved with plastic. Hadron showers are produced in the absorber (brass) and scintillation light is produced in the active material (plastic) as the shower passes through. The solenoid lies outside of the HCAL and provides a 3.8 T axial magnetic field. Embedded in the iron return yoke of the magnet sit the muon

systems. Three different types of muon detectors are used to identify muons and make momentum and charge measurements over a large kinematic range.

Crucial to the successful operation of CMS is the trigger. The pp interaction cross section is 100 mb, while for example, the W boson production cross section is some 6 orders of magnitude less than this, and the rare physics processes that CMS was built to search for, such as Higgs boson and SUperSYmmetry (SUSY) production, many times smaller still. The LHC delivers an unprecedented high instantaneous luminosity so that such rare physics processes occur, but this also implies that the vast majority of the collisions result in 'uninteresting' physics: namely Quantum Chromo-Dynamics (QCD) processes. It would be impossible to record such high volumes of data that comes out of CMS, some PB s^{-1}, and not useful to do so. Therefore, a very efficient method of recording those events that appear 'interesting' is necessary, to reduce the 40 MHz event rate to a more manageable 100 Hz. The two-tier trigger system fulfills this role, via a hardware based online Level 1 Trigger (L1) an software based offline Higher Level Trigger (HLT).

More information on the CMS detector can be found in Ref. [3].

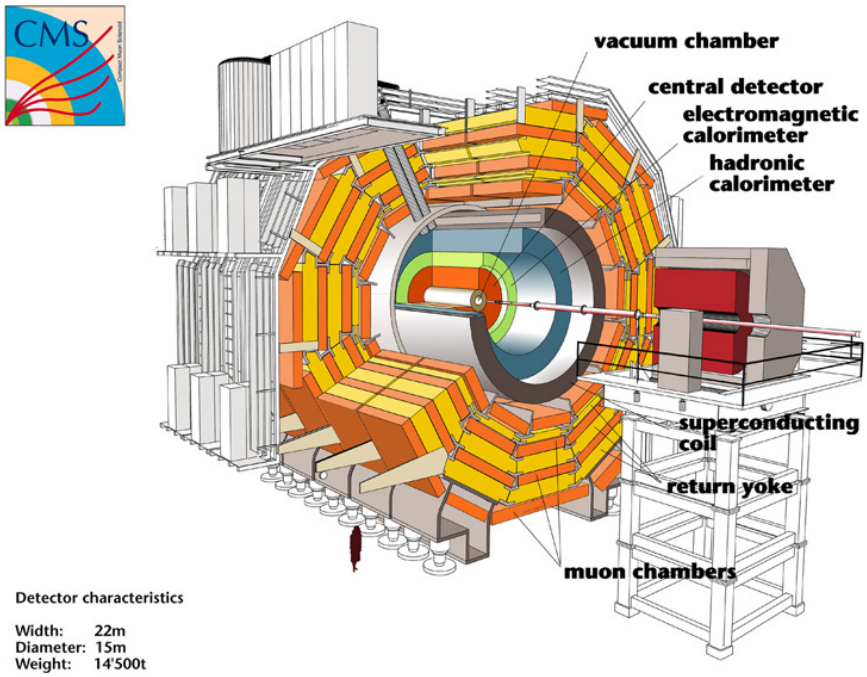

Figure 3.2.: The CMS detector, with the main subsystems labelled.

CMS uses a right-handed coordinate system; the x-axis points south towards the centre of the LHC ring, the y-axis points vertically upwards and the z-axis is in the

direction of the beam, where positive z is to the west. More useful is the cylindrical coordinate system, defined in terms of r, ϕ and θ. The azimuthal angle ϕ is measured from the x-axis in the xy plane, where the radial component is denoted r. The polar angle θ is defined in the rz plane, and the pseudorapity

$$\eta = -\ln\tan(\theta/2). \tag{3.1}$$

Convention is that the position of a particle is described in terms of η and ϕ, where $\eta = 0$ is along the y-axis and $\eta = \infty$ is along the beam direction; and $-\pi < \phi < \pi$. The distance between particles is commonly described in terms of the variable $\Delta R = \sqrt{\Delta\phi^2 + \Delta\eta^2}$.

The LHC is a hadron collider, and as such, collides non-fundamental particles. Inelastic collisions with large momentum transfer can occur between component quarks and gluons, however in a single bunch crossing there will also be many low energy, elastic, soft scatters, as well as the remnant part of any protons that have had a hard collision. As a result, the forward and backward directions are highly radiative environments and therefore difficult to instrument due to high occupancy and radiation damage. CMS has endcaps to extend the detector coverage at high η, however it is not possible to reconstruct momentum of a single interaction in the direction of the beam. Additionally, interesting physics is a result of a hard collision, where energy is available for the creation of new particles. It can be characterized by the amount of energy in the transverse (xy) plane. For these reasons, particle energy and momenta are described only in the transverse plane, where conservation laws can be applied. By conserving energy and momentum in the transverse plane, any imbalance can be assigned to a particle leaving the detector without any trace; for example from a neutrino, or, from new physics processes such as Dark Matter (DM) production. 4π particle reconstruction and measurements of missing transverse energy, the 'tell-tale' sign of new physics, makes CMS perfectly suited to searching for physics beyond the SM.

3.2.1. The Tracking System

The tracker is designed for precise and efficient measurement of charged particle trajectories (and therefore position and momentum) as they emerge from the interaction point. Additionally, reconstruction of any secondary vertices is crucial for identifying heavy flavor decays such as jets that originate from b-quarks.

The LHC provides bunch crossings every 25 or 50 ns, resulting in $\sim$ 20 pp interactions, giving rise to of order 1000 particles. All of these traverse the tracker. The granularity of the tracker must be such that one can determine which of the $\sim$ 20 pp vertices each of the particles come from, and the electronics fast enough that the information is sent on in time for the next bunch crossing to arrive. With such high particle fluxes, the tracker is also subject to a huge amount of radiation damage. These conditions must be dealt with using the least amount of material possible in order to limit multiple scattering, photon conversion, bremsstrahlung and nuclear interactions. To meet with such criteria, and to have an estimated lifetime of 10 years, the tracker is constructed entirely from silicon.

The tracker consists therefore of an all silicon pixel and strip detector. Measuring 5.8 m in length and 2.5 m in diameter, with a total active area of 200 m^2, it surrounds the interaction region. The pixel detector has three layers in the barrel, at radii of 4.4 cm, 7.3 cm and 10.2 cm. In the endcaps, there are two disks at distances $z = \pm 34.5, \pm 46.5$ cm. The strip detector has a length of 5.8 m and a diameter of 2.4 m, and is composed of four subsystems: the Tracker Inner Barrel (TIB), Tracker Outer Barrel (TOB), Tracker Inner Disks (TID) and Tracker Endcaps (TEC). The CMS tracker geometry is shown in Figure 3.3.

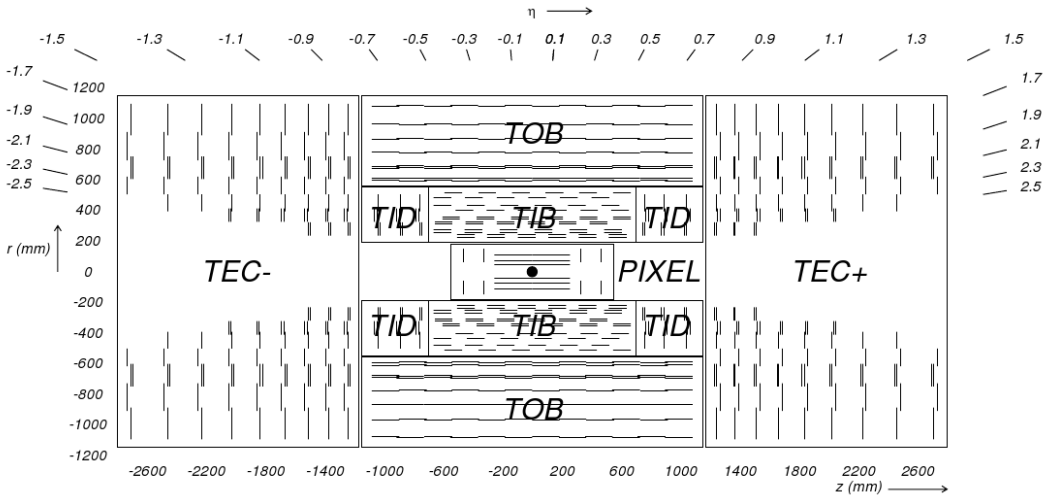

Figure 3.3.: The CMS tracker, shown in the rz plane. The pixel detector is shown at the centre of the tracker, closest to the interaction region (shown by the black dot), and the strip detector surrounds it. The different subsystems of the strip detector are shown, taken from Ref. [3].

3.2.2. The Electromagnetic Calorimeter

High resolution photon and electron position and energy measurements are provided by the lead tungstate ($PbWO_4$) crystal ECAL, which covers pseudorapidty up to $|\eta| < 3$. It is made up of the Electromagnetic Calorimeter Barrel (EB), covering the range $0 < |\eta| < 1.479$, and the Electromagnetic Calorimeter Endcap (EE), covering the range $1.479 < |\eta| < 3$.

Both fast response times (80% of scintillation light is emitted in 25 ns) and radiation hardness are required from the ECAL, motivating the choice of material. In addition, it is very dense (8.28 gcm^{-1}), has a short radiation length ($X_0 = 0.89$ cm), and small Molière radius (2.2 cm), making it well suited to a compact, fine granularity calorimeter. 61,200 crystals in the barrel and 7,324 crystals in the endcaps are tapered in shape and arranged in a quasi-projective geometry, angled at 3° to ensure that particle trajectories avoid cracks between them. Barrel crystals have a front face of 22×22 mm^2 and a length of 23 cm, corresponding to 25.8 X_0. Endcap crystals have a front face of 28.6×28.6 mm^2 and length corresponding to 24.7 X_0. Electromagnetic showers are therefore expected to be contained within one crystal length, so only a single layer of crystals is needed. A preshower detector is place in front of the endcaps, with a thickness of $3X_0$, in the range $1.653 < |\eta| < 2.6$, in order to distinguish between single photons and photon pairs resulting from neutral pion decay. The ECAL geometry is shown in Figure 3.4.

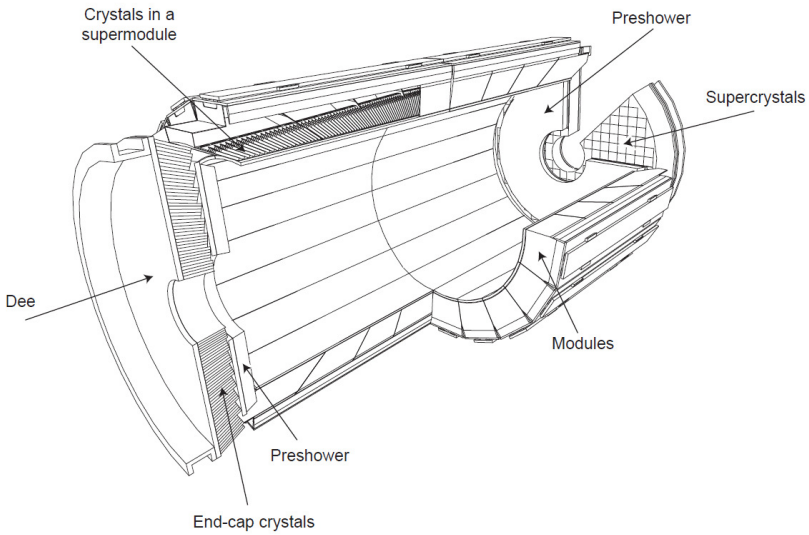

Figure 3.4.: Geometric view of the CMS ECAL. Barrel crystals are arranged in modules and supermodules, and endcap crystals arranged in supercrystals. Also shown is the preshower detector.

The very dense material $PbWO_4$ causes incident photons and electrons to shower. Resulting pair produced electrons and positrons, and radiated photons, cause scintillation light in the transparent, polished crystals. The amount of light produced is proportional to the incident particle energy, and is collected by an Avalanche Photo-Diodes (APD) on the end of each crystal in the barrel, and Vacuum Photo-Triodes (VPT) in the endcaps. These photodetectors also have to be radiation hard and operate successfully in the 3.8 T magnetic field, while providing significant amplification to signal. Both the crystal and photodetector performance has a strong temperature dependence, so the ECAL is kept at a constant temperature of 18° via a water cooling system, and is stable to ± 0.05 °C.

3.2.3. The Hadronic Calorimeter

The HCAL provides complementary energy measurements of hadronic showers, crucial for measuring jets and missing transverse energy. It is a sampling brass calorimeter, built from alternating layers of large, absorbing brass plates, interleaved with scintillating plastic tiles arranged in trays. Sitting within the bore of the solenoid, the Hadron Barrel (HB) covers pseudorapidity $|\eta| < 1.3$, and the Hadron Endcaps (HE) on each side enclose $1.3 < |\eta| < 3$. To attain a most hermetic detector, there is also a Hadron Forward (HF), which extends coverage right up to $|\eta| < 5.2$.

The quality of the HCAL's measurements is dictated by the fraction of the hadronic shower that passes through the scintillator; the plastic must be thick enough to catch the majority of the shower. This demand for radial extension is at odds with the location of the HCAL, from the outer edge of the ECAL at $r = 1.77$ m, and the inner edge of the solenoid at $r = 2.95$ m. Providing a compromise, an outer hadronic calorimeter, Hadron Outer (HO), is placed outside of the vacuum tank of the magnet and supplements the HB. Using the solenoid coil as absorber material, it can identify late starting showers, providing sufficient containment for 11.8 interaction lengths (λ_L). Five rings of HO are arranged along the z-axis of the detector, where the central ring at $\eta = 0$ has two layers at $r = 3.82$ m and 4.07 m, and the rest have a single layer at $r = 4.07$ m. Figure 3.5 shows the geometry of the HCAL.

Hadron showers are created in the brass absorber plates, through nuclear interactions in the material, and the plastic scintillator tiles produce blue-violet light when the shower passes through. It is read out using wavelength shifting fibres, sending the now green light down transparent fibres to Hybrid Photodetectors (HPD) which produce an electrical signal proportional to the incident hadron energy. The first layer of plastic tiles are

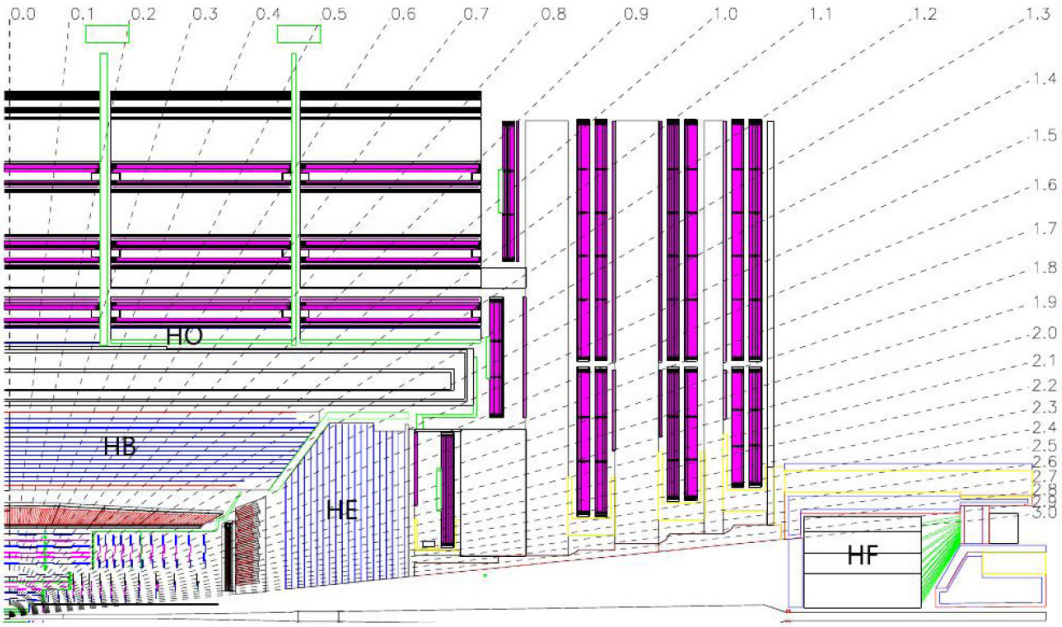

Figure 3.5.: Longitudinal view of the CMS HCAL. Locations of the HB, HO, HE and HF are shown with values of η. The purple regions represent the muon detectors which further restrict the volume of the HO.

placed in front of the first absorber plate in order to sample the incoming shower as it develops in the material between the ECAL and the HCAL. The final layer of scintillator placed after the final brass plate to catch any late developing showers. 70,000 plastic scintillator tiles are in the HB and 20,916 tiles are in the HE.

The HF uses different technology in order to cope with the much harsher environment in which it is situated. With an average energy of 760 GeV deposited in the HF per pp collision at LHC design energy, peaking at the highest rapidity point closest to the beam line, radiation hardness and occupancy requirements demand alternative materials. Steel absorber plates are embedded with scintillating quartz fibres, which act to detect the Cherenkov light emitted by charged particles in the shower. It is therefore most sensitive to the electromagnetic component of the shower.

3.2.4. The Muon System

Muons are a powerful tool for recognising signs of interesting physics. A relatively easy experimental signature to identify, muons can provide excellent 2- or 4-particle mass resolutions as they do not suffer from radiative losses (as electrons do). Excellent muon reconstruction is therefore a central design feature. Embedded in the iron flux-return

yoke of the solenoid, the muon systems combine three methods of gaseous detection to identify, carry out high resolution momentum measurements, and trigger events, up to $|\eta| < 2.4$.

In the barrel ($|\eta| < 0.9$), magnetic flux is concentrated in the iron return yoke so residual field is very small. There is also a low muon rate and neutron induced background, so Drift Tube (DT) chambers are used. In the endcaps ($0.9 < |\eta| < 2.4$), magnetic field and muon rate are much higher, so Cathode Stripe Chambers (CSCs) are used instead; they have a faster response time, higher granularity and better radiation hardness. Both the DT and CSCs have excellent position resolution. An additional system of Resistive Plate Chambers (RPCs) in both the barrel and endcaps provide an independent signal which has both good time resolution (and poorer position resolution) and serves as a trigger.

By combining information from the tracker, and from either the DT or CSCs and RPCs, CMS has excellent muon reconstruction. Precise momentum resolution is achieved for the whole kinematic range, from 10 GeV to > 500 GeV, shown in Figure 3.6.

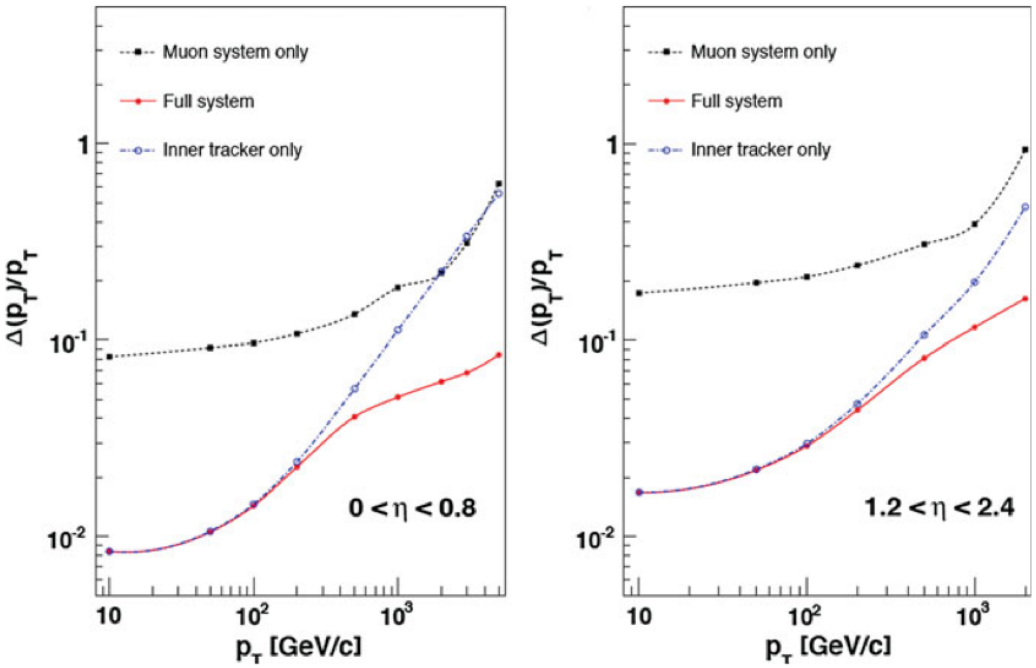

Figure 3.6.: Muon transverse momentum resolution, shown as a function of muon p_T in the barrel (left) and the endcaps (right). The resolution of the tracker and muon systems is shown, and the enhancement gained by combining the information.

3.2.5. The Trigger

Chapter 4.

Jet Algorithms for the L1 Trigger Upgrade

Here are some funky floats using "continued captions", i.e. for a semantically collected group of float contents which are too numerous to fit into a single float, such as the pretty circles in the following figure:

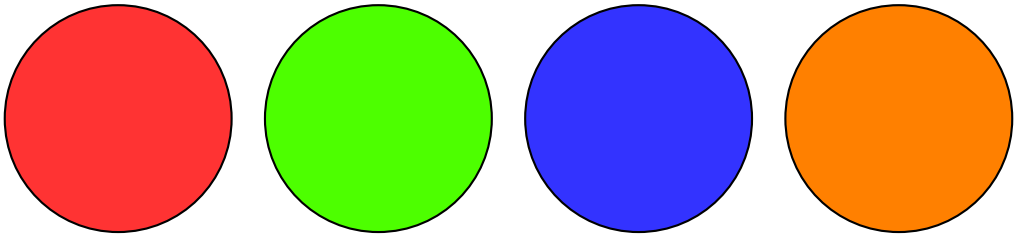

(a) Example 1a **(b)** Example 1b **(c)** Example 1c **(d)** Example 1d

Figure 4.1.: Demonstration of `subfig` continued captions.

This mechanism means that the same float label is used for both pages of floats. Note that we can refer to Figure 4.1 in general, or to Figure 4.1g on page 17 in particular!

Just for the hell of it, let's also refer to Section **??**.

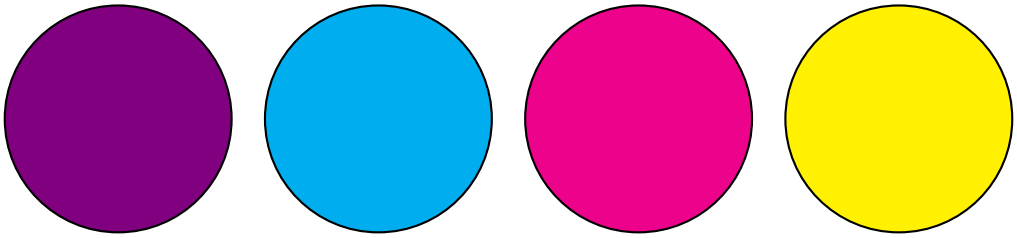

(e) Example 1e **(f)** Example 1f **(g)** Example 1g **(h)** Example 1h

Figure 4.1.: Demonstration of `subfig` continued captions (continued).

Chapter 5.

Searching for Compressed SUSY with monojet events

"There, sir! that is the perfection of vessels!"
— Jules Verne, 1828–1905

5.1. Analysis

cp PAS.tex .

Appendix A.

Pointless extras

« *Le savant n'étudie pas la nature parce que cela est utile;*
il l'étudie parce qu'il y prend plaisir,
et il y prend plaisir parce qu'elle est belle. »
— Henri Poincaré, 1854–1912

Appendixes (or should that be "appendices"?) make you look really clever, 'cos it's like you had more clever stuff to say than could be fitted into the main bit of your thesis. Yeah. So everyone should have at least three of them...

A.1. Like, duh

Padding? What do you mean?

A.2. $y = \alpha x^2$

See, maths in titles automatically goes bold where it should (and check the table of contents: it *isn't* bold there!) Check the source: nothing needs to be specified to make this work. Thanks to Donald Arsenau for the teeny hack that makes this work.

Bibliography

[1] K. Aamodt, et al., The ALICE experiment at the CERN LHC, JINST 3 (2008) S08002. doi:10.1088/1748-0221/3/08/S08002.

[2] G. Aad, et al., The ATLAS Experiment at the CERN Large Hadron Collider, JINST 3 (2008) S08003. doi:10.1088/1748-0221/3/08/S08003.

[3] S. Chatrchyan, et al., The CMS experiment at the CERN LHC, JINST 3 (2008) S08004. doi:10.1088/1748-0221/3/08/S08004.

[4] J. Alves, A. Augusto, et al., The LHCb Detector at the LHC, JINST 3 (2008) S08005. doi:10.1088/1748-0221/3/08/S08005.

List of Figures

List of Tables

1. Acronyms

ALICE	A Large Ion Collider Experiment
ATLAS	A Toroidal LHC ApparatuS
APD	Avalanche Photo-Diodes
BSM	Beyond Standard Model
CERN	European Organisation for Nuclear Research
CMS	Compact Muon Solenoid
CMSSM	Compressed Minimal SuperSymmetric Model
CSCs	Cathode Stripe Chambers
CSV	Combined Secondary Vertex
CSVM	Combined Secondary Vertex Medium Working Point
DM	Dark Matter
DT	Drift Tube
ECAL	Electromagnetic Calorimeter
EB	Electromagnetic Calorimeter Barrel
EE	Electromagnetic Calorimeter Endcap
ES	Electromagnetic Calorimeter pre-Shower
EMG	Exponentially Modified Gaussian

EPJC European Physical Journal C

EWK Electroweak Sector

GCT Global Calorimeter Trigger

GMT Global Muon Trigger

GT Global Trigger

HB Hadron Barrel

HCAL Hadronic Calorimeter

HE Hadron Endcaps

HF Hadron Forward

HLT Higher Level Trigger

HO Hadron Outer

HPD Hybrid Photodetectors

ISR Initial State Radiation

LUT Look Up Table

L1 Level 1 Trigger

LEP Large Electron-Positron Collider

LHC Large Hadron Collider

LHCb Large Hadron Collider Beauty

LO Leading Order

LSP Lightest Supersymmetric Partner

NLL Next to Leading Logorithmic Order

NLO Next to Leading Order

NNLO Next to Next Leading Order

POGs Physics Object Groups

PS Proton Synchrotron

QED	Quantum Electro-Dynamics
QCD	Quantum Chromo-Dynamics
QFT	Quantum Field Theory
RBXs	Readout Boxes
RPCs	Resistive Plate Chambers
RCT	Regional Calorimeter Trigger
RMT	Regional Muon Trigger
SUSY	SUperSYmmetry
SM	Standard Model
SMS	Simplified Model Spectra
SPS	Super Proton Synchrotron
TIB	Tracker Inner Barrel
TEC	Tracker Endcaps
TID	Tracker Inner Disks
TOB	Tracker Outer Barrel
TF	Transfer Factor
TP	Trigger Primitive
VEV	Vacuum Expectation Value
VPT	Vacuum Photo-Triodes
WIMP	Weakly Interacting Massive Particle